J Mater Sci (2007) 42:2637–2642
DOI 10.1007/s10853-006-1350-7

Microstructure and electrical properties of ZnO-based varistors prepared by high-energy ball milling

Hong-Yu Liu · Hui Kong · Xue-Ming Ma · Wang-Zhou Shi

Received: 8 July 2005 / Accepted: 28 February 2006 / Published online: 4 January 2007

Abstract ZnO-based varistor ceramics were prepared at sintering temperatures ranging from 900 °C to 1,300 °C, by subjecting the mixed oxide powders to high-energy ball milling (HEBM) for 0, 5, 10 and 20 h, respectively. Varistor ceramics prepared by HEBM featured denser body, better electrical properties sintered at low-temperature than at traditional high-temperature. The high density is due to the refinement of the crystalline grains, the enhanced stored energy in the powders coming from lattice distortion and defects as well as the promotion of liquid-phase sintering. Good electrical properties is attributed to proper microstructure formed at low-temperature and improved grain boundary characteristics resulting from HEBM. With increasing sintering temperatures, the electrical properties and density became worse due to the decrease in amount of Bi-rich phase. Temperature increased up to 1,200 °C or above, the Bi-rich phase vanished and the ceramics exhibited very low nonlinear coefficient.

H.-Y. Liu · H. Kong · X.-M. Ma (✉) · W.-Z. Shi
Department of Physics, East China Normal University, 3663 North Zhongshan Road, 200062 Shanghai, China
e-mail: xmma@phy.ecnu.edu.cn

X.-M. Ma
Key Laboratory of Optical and Magnetic Resonance Spectroscopy of Ministry of Education, 3663 North Zhongshan Road, 200062 Shanghai, China

Introduction

ZnO-based varistors are widely used as surge absorbers in electrical power systems and electronic circuits to protect against dangerous over-voltage surges, due to their nonlinear current–voltage characteristics and a high energy-absorption capability. In lightning arrester field, for reducing element weight and sizes, Japan developed high voltage-gradient arresters of 400 V/mm in electrical power system [1–4]. Many researchers prepared high voltage-gradient ZnO varistors by using chemical methods. Lauf [5] fabricated 980 V/mm varistors through sol–gel processing. Viswanath [6] prepared varistors for voltage-gradient up to 3,000 V/mm by colloidal suspension and centrifugal separation method at sintering temperature of 750 °C. Duran [7] also employed nanometer size powder produced by chemical method to fabricate ZnO varistors for voltage-gradient of 2,000 V/mm through two-stage thermal processing method, first and second stage is 900 °C and 825 °C, respectively. Those methods have the disadvantages of complicated process, high production costs and hardly be adopted in commercial production. Recently, a method of high-energy ball milling (HEBM), changing original powder from micro into nanometer size, was employed by Fah [8] and Alamdari [9] to produce high voltage-gradient varistors. Although their sintering temperatures were reduced to 1,100, 1000 °C to research, respectively, they neither correlate ceramics properties including density, voltage-gradient (V_{1mA}/mm), nonlinear coefficient (α) and leakage current (I_L) with sintering temperatures nor detailed the mechanism of low-temperature sintering associated with HEBM, which will be most attractive both in industry application and scientific research. The purpose

of this paper is to correlate sintering temperature with microstructure, density and electrical properties of varistor ceramics prepared by HEBM and try to reveal the mechanism of low-temperature sintering.

Experimental

The composition of 96.5 mol% ZnO, 0.7 mol% Bi_2O_3, 1.0 mol% Sb_2O_3, 0.8 mol% Co_2O_3 and 0.5 mol% each of Cr_2O_3 and MnO_2 was chosen for investigation. The commercially available ZnO powder was milled together with additives in ethanol in nylon jars using stainless steel balls as the milling media in a planetary high-energy ball mill operated at 500 rpm. The ratio of balls to mixed powder was fixed at 20:1. The mixture was milled for 5–20 h, followed by drying the slurry at 200 °C. The as-dried powder mixture was milled again for 1 h to eliminate large powder lumps. The resulting powder was uniaxially pressed into discs of 10 mm in diameter and 2 mm in thickness by an universal hydraulic presser. Sintering of the discs was carried out in air in a resistance furnace at various temperatures ranging from 900 °C to 1,300 °C for 2 h, with heating rate fixed at 5 °C/min and cooling in furnace.

The powder mixtures with and without HEBM, the sintered discs were characterized using X-ray diffractometer (XRD, D/max 2550V, Cu-Kα). The crystalline grain size of milled powder was calculated by applying the Scherrer equation [10], crystalline size = $0.9\lambda/(B\cos\theta)$, whereλ = X-ray wavelength, θ = Bragg angle, B = full width at half maximum (FWHM). The contamination (Fe element) to powder mixtures coming from steel balls was analyzed by Inductively Coupled Plasma-Atomic Emission Spectrometry (ICP-AES, Plasma2000). The density of sintered discs was measured using the Archimedes'method in distilled water.

For DC current–voltage characterization, silver electrodes were painted on both surfaces of the discs and fired at 600 °C in air. The varistor voltage at 1 and 0.1 mA were measured and the voltage-gradient V_{1mA}/mm and nonlinear coefficient α were determined ($\alpha = 1/\lg(V_{1mA}/V_{0.1mA})$). The leakage current I_L was measured at 0.75 V_{1mA}. The donor concentration N_d, barrier height ϕ_B, density of interface states N_s and the barrier width ω were determined by using a grain-boundary defect model [11–13], according to which, the electric conduction in the ohmic region was associated with the thermion emission of Schottky type, i.e., emission current density

$$J = A * T^2 \exp\left[\left(\beta E^{1/2} - \Phi_B\right)/kT\right], \quad (1)$$

where A^* is Richardson constant ϕ_B is the potential barrier height formed at the interface, E is the electric field, K is boltzmann constant, T is absolute temperature and β is a constant related to the potential barrier width by the relationship

$$\beta = \left[(1/(r * \omega))\left(2e^3/(4\pi\varepsilon_0\varepsilon_r)\right)\right]^{1/2}, \quad (2)$$

where r^* is the number of grains per unit length, ω is the barrier width, e is electron charge, ε_0 is vacuum dielectric constant (8.85×10^{-14} F/cm), ε_r is relative dielectric constant (8.5 for ZnO). Fixing T at room temperature, plotting ln$J$ versus $E^{1/2}$ for some samples, the ϕ_B can be obtained from the intersections of the extrapolated regression lines with the ln$J$ axis and the constant β can be derived from the slopes of the plots. Knowing the values of r^* by SEM measurement, the ω can be obtained from the Eq. (2). Then N_d can be derived from the equation [14] $\omega^2 = (2\phi_B\,\varepsilon_0\varepsilon_r)/(e^2\,N_d)$ and the N_s from $N_s = N_d\omega$.

The sintered discs' microstructures were examined using a scanning electron microscopy (SEM, JEOL, JSM-6360LV) in back-scattered electron mode. The phase compositions of the samples were determined by energy-disperse X-ray spectroscopy (EDX, EDAX, FALCON) on the SEM. The average ZnO diameter (D) was measured of each recognizable grain in a certain area, and the average of 100 grains was calculated without correction factors.

Results and discussion

XRD data of the powders that was subjected to 5, 10 and 20 h of HEBM and that was not subjected to any HEBM are shown in Table 1. It can be seen that the FWHM of ZnO increased with increasing milling time. ZnO crystalline size, calculated from Scherrer equation, was refined from ~120 nm to ~59 nm by 20 h of HEBM, and the refinement speed gradually decreased with increasing milling time.

In Fig. 1, the voltage-gradient is plotted against the sintering temperature. It is distinct that the voltage-gradient of milled samples is higher than that of unmilled ones at all sintering temperatures. From the

Table 1 Change of ZnO crystalline size and FWHM with the time of HEBM

Milling time (h)	0	5	10	20
FWHM of ZnO(100)	0.179	0.210	0.243	0.250
ZnO crystalline size (nm)	120	83	62	59

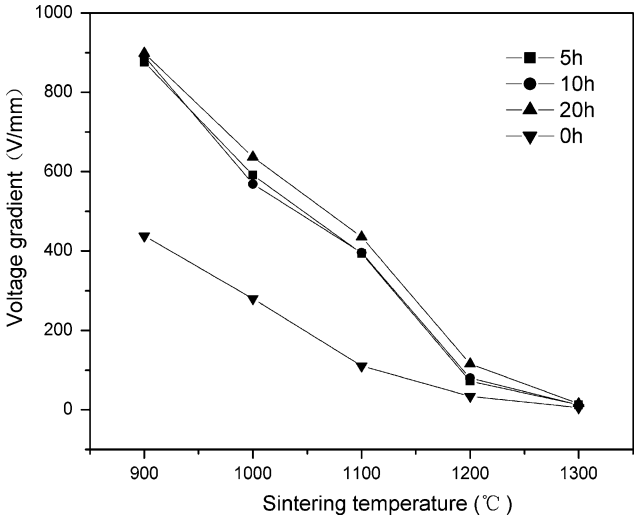

Fig. 1 The relationship between voltage-gradient and sintering temperature for samples derived from the powders subjected to 0, 5, 10 and 20 h of HEBM

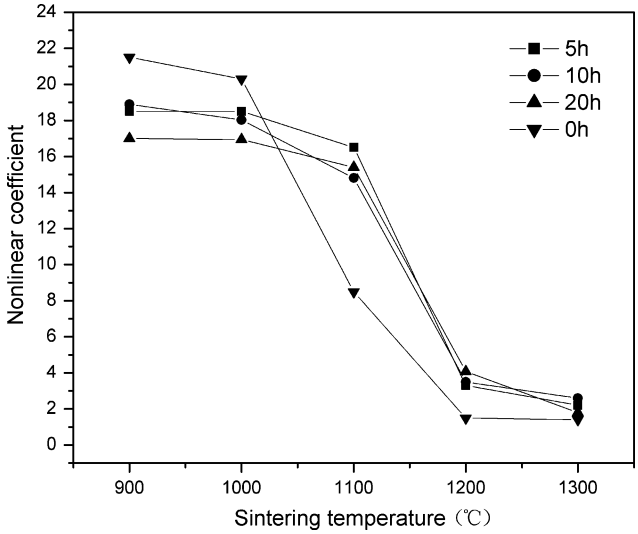

Fig. 2 The relationship between nonlinear coefficient and sintering temperature for samples derived from the powders subjected to 0, 5, 10 and 20 h of HEBM

formula [15] $E_S = nV_b$, where E_S is the breakdown field, n the number of schottky barriers per unit length along the direction of current conduction and V_b, whose values does not much vary from one barrier to another and has a range of 2–4 V, the voltage drop at each barrier, it can be seen that E_S mainly depends on n values. With sintering temperatures increasing from 900 °C to 1,300 °C, grain size of sample increases markedly resulting in reduced n and so E_S value. E_S at temperature of 900 °C lies in the region of 875–898 V/mm. The increase in voltage-gradient with increasing milled time (0–20 h) at a fixed temperature is due to the refined grain size [8], obtained as a result of HEBM. According to Fig. 1, a relatively high voltage-gradient of 400 V/mm and above can be obtained when a nanocrystalline powder prepared by HEBM is sintered at 1,100 °C and below.

Figure 2 shows the effect of the sintering temperature on the α of samples derived from the powders subjected to 0, 5, 10 and 20 h of HEBM. It can be seen that α for milled samples, keeps decreased with temperature increasing, changing little at temperature 900–1,100 °C, but drastically decreases from 1,100 °C to 1,200 °C and then continuously decreases slowly. This is attributed to a lowering of the grain boundary barrier height with increasing sintering temperatures [16]. For unmilled samples, α is higher than milled ones during 900–1,000 °C, then decreases rapidly and becomes smaller than milled samples at sintering temperatures of 1,100–1,300 °C.

Figure 3 shows the effect of the sintering temperature on the I_L of samples derived from the powders

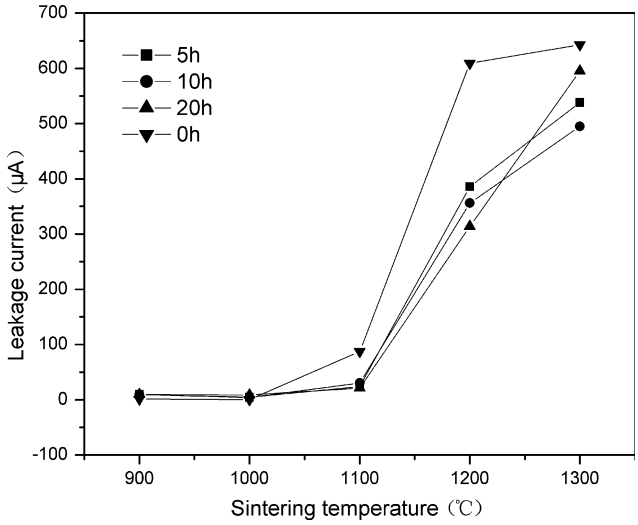

Fig. 3 The relationship between leakage current and sintering temperature for samples derived from the powders subjected to 0, 5, 10 and 20 h of HEBM

subjected to 0, 5,10 and 20 h of HEBM. Contrary to α change, I_L increases when sintering temperature increases. It changes also little during 900–1,100 °C, but going up rapidly from 1,100 °C to1200 °C, then rising slowly again. Leakage currents of unmilled samples become greater than milled ones at 1,000 °C, from which the α of unmilled samples become smaller than milled ones (Fig. 2). It seems that I_L change is correlated with α. According to equation (1), it's apparent that emission current, i.e., leakage current, increases with decreasing ϕ_B due to increasing sintering temperature.

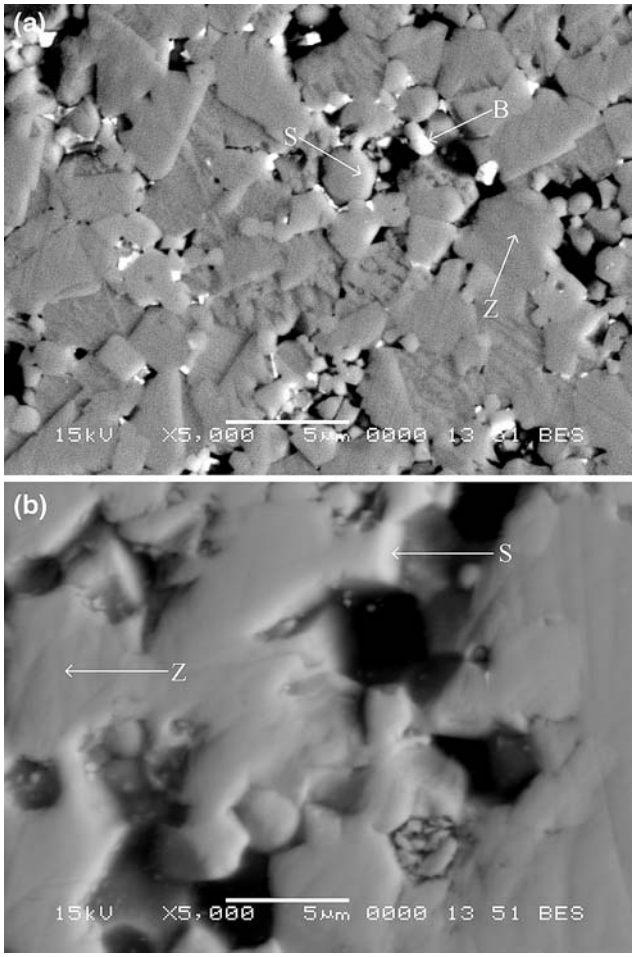

Fig. 4 Backscattered electron images of varistor ceramics sintered at 900 °C (**a**) and 1,200 °C (**b**) for 2 h, derived from mixed powders that were subjected to HEBM for 5 h

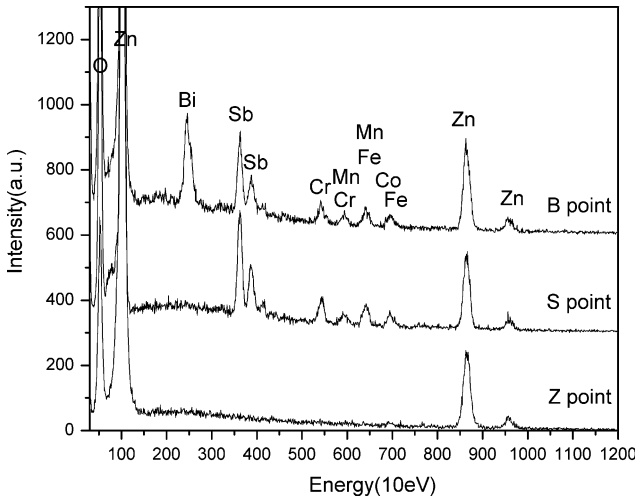

Fig. 5 EDX analysis of marked points in Fig. 4

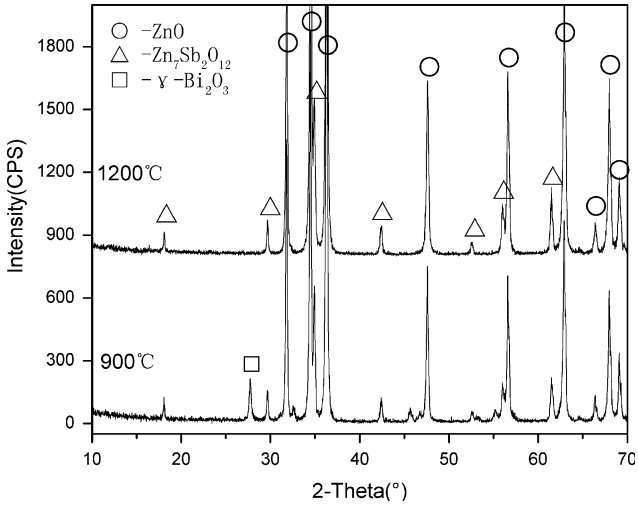

Fig. 6 XRD patterns of varistor ceramics sintered at 900 °C and 1,200 °C for 2 h, derived from mixed powders that were subjected to HEBM for 5 h

The SEM micrograph and EDX of samples sintered at 900 °C and 1,200 °C, derived from mixed powders that were subjected to HEBM for 5 h, are shown in Figs. 4 and 5, respectively. There are four noticeable regions, white, offwhite, gray and black, in the sample sintered at 900 °C. The white regions (B points) are identified by EDX as Bi-rich phase, the offwhite regions (S points) are spinel phases, the gray regions (Z points) are ZnO phases (Fig. 5) and the black regions are pores. In sample sintered at 1,200 °C, however, the white regions in which Bi-rich phase exists disappear, existing phases are ZnO and spinel (Fig. 4b). Figure 6 shows the XRD patterns of samples sintered at 900 °C and 1,200 °C for 2 h, derived from mixed powders that were subjected to HEBM for 5 h. Samples sintered at 900 °C are composed of ZnO + $Zn_7Sb_2O_{12}$ + γ-Bi_2O_3, the samples sintered at 1,200 °C just have ZnO + $Zn_7Sb_2O_{12}$, no existence of γ-Bi_2O_3. These results indicate Bi-rich phases have already vaporized after sintered at 1,200 °C. Because Bi-rich phase, ~2 nm intergranular amorphous Bi-rich film and intergranular segregated Bi atoms are the key phases which exhibit higher barrier voltages and lead to high α values [17], no Bi-rich phase or very little should be the reason why steep change of α values (Fig. 2) and the I_L rapid increase (Fig. 3) when samples sintered at 1,100–1,200 °C.

The relative density of the sintered samples derived from the powders subjected to 0, 5, 10 and 20 h of HEBM at various sintering temperatures is plotted in Fig. 7. For all samples derived from the powders subjected to 0, 5, 10 and 20 h of HEBM, the density decreases with the sintering temperature increasing

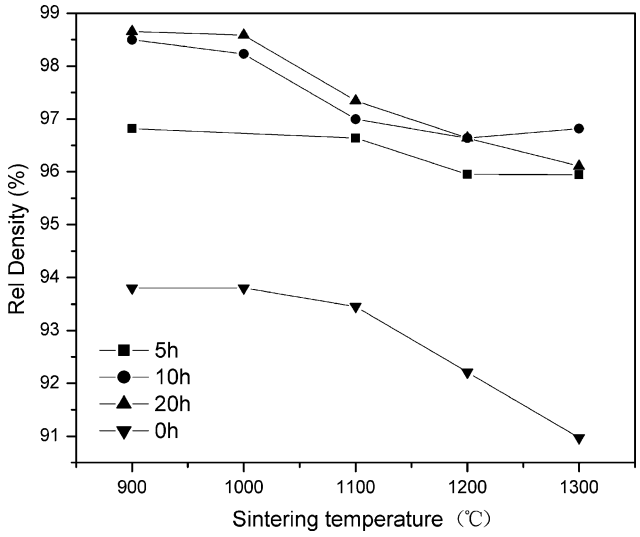

Fig. 7 Relative density of the samples derived from the powders subjected to 0, 5, 10 and 20 h of HEBM as a function of sintering temperature

from 900 °C to 1,300 °C. This result is consistent with literature [18]. As mentioned above, the decrease or vanishment in amount of Bi_2O_3, whose density (8.9 g/cm^3) is greater than ZnO (5.6 g/cm^3), leads to the decrease in density with increasing sintering temperature.

Before sintered and after uniaxially pressed under the same pressure of 98 kN, the density of the samples derived from the powders subjected to 5, 10 and 20 h of HEBM are 5.54, 5.36, 5.22 g/cm^3, respectively. The trend of density change is that the more time the sample powder was milled, the smaller is its green disc density. This is because the more time milled samples have smaller particles and produce more voids full of air after pressed under the same pressure, resulting in lower density of green disc. However, after sintered at various temperatures, the density magnitude order is changed reversely, i.e., the trend of density altering is that the more time the sample powder was milled, the higher is its density of sintered disc (the only exception is the sample, which is milled 10 h and sintered at 1,300 °C). This comes from the following reasons: (1) HEBM has a promoted effect on the sintering densification behavior. HEBM caused the refinement of the crystalline sizes of ZnO and other constituters, the enhanced stored energy in the powders due to lattice distortion and defects, which are responsible for the increase of the sintering driving force and kinetics factor and the shortening of the elemental diffusion distance. (2) At the sintering temperatures ranging from 900 °C to 1,300 °C, Bi_2O_3 and Sb_2O_3 are liquid, and the densification is governed by liquid-phase sintering process. Liquid phases increase the contacted area between reactant phases, accelerate the transmission speed, promote the reaction among reactant phases and make ceramics more denser. (3) More time milled samples accepted more contamination elements like Fe (the concentration of Fe in 5, 10, and 20 h milled powders is 0.78, 0.99, 1.39 wt%, respectively), whose density is higher than ZnO.

In order to explore the electrical conduction behavior of HEBM sample sintered at low-temperature of 900 °C, we used a grain-boundary defect model and relative equations (mentioned in experimental part) and obtained the values of calculated ϕ_B, ω, N_d and N_s, shown in Table 2. It can be seen that N_d, N_s and ϕ_B, of milled samples, increases and ω decreases when the milling time increases. The more time the samples milled, the more noticeable are the above trends. This might be caused by the more crystal lattice distortion and defects produced during HEBM, which led to higher donor concentration and density of interface states.

Conclusions

Varistor ceramics prepared by HEBM featured denser body, better electrical properties sintered at low-temperature than at traditional high-temperature. The high density is due to the refinement of the crystalline grains, the enhanced stored energy in the powders coming from lattice distortion and defects as well as the promotion of liquid-phase sintering. Good electrical properties is attributed to proper microstructure

Table 2 Some characteristics of the samples sintered at 900 °C for 2 h, derived from mixed powders that were subjected to HEBM for 0, 5, 10 and 20 h

Milling time, t (h)	crystalline size, D (μm)	Barrier height, φ_B (eV)	Barrier width, ω (nm)	Donor concentration, N_d (10^{18}cm^{-3})	Density of interface states, N_s (10^{12}cm^{-2})
0	7.7	0.80	553	0.0025	0.14
5	3.6	0.97	9.59	9.84	9.44
10	2.9	1.02	5.56	31.05	17.25
20	2.2	1.04	3.87	64.99	25.15

formed at low-temperature and improved grain boundary characteristics resulting from HEBM. With increasing sintering temperatures, the electrical properties and density became worse due to the decrease in amount of Bi-rich phase. Temperature increased up to 1,200 °C or above, the Bi-rich phase vanished and the ceramics exhibited very low nonlinear coefficient. The donor concentration N_d, density of interface states N_s, barrier height ϕ_B increased but the barrier width ω decreased with increasing milling time for samples sintered at 900 °C.

Acknowledgements This work was supported by National Natural Science Foundation of China (Grant No.50471045) and Shanghai Nano-technology Promotion Center (Grant No.0452nm026).

References

1. Shirakawa S, Ejiri I, Watahiki S (1999) IEEE T Power Deliver 14:419
2. Shichimiya S, Yamaguchi M, Furuse N (1998) IEEE T Power Deliver 13:465
3. Shirakawa S, Yamada S, Tanaka S (2000) IEEE T Power Deliver 15:569
4. Imai T, Udagawa T, Ando H (1998) IEEE T Power Deliver 13:1182
5. Lauf Robert J, Bond Walter D (1984) Ceram Bull 63:278
6. Viswanath RN, Ramasamy S, Ramamoorthy R (1995) Nanostruct Mater 6:993
7. Duran P, Capel F, Tartaj J, Moure C (2002) Key Eng Mater 206–213:1389
8. Fah CP, Wang J (2000) Solid State Ionics 132:107
9. Alamdari HD, Boily S, Blouin M (2000) Mater Sci Forum 343–346:909
10. Pillai SC, Kelly JM, McCormack DE (2004) Mater Sci Tech 20:964
11. Pianaro SA, Bueno PR, Olivi P (1997) J Mater Sci Lett 16:634
12. Pianro SA, Bueno PR, Longo E, Varela JA (1998) J Mater Sci: Mater Electron 9:159
13. Li Changpeng, Wang Jinfeng, Su Wenbin (2001) Physica B 307:1
14. Morris William G (1976) J Vac Sci Technol 13:926
15. Bui A, Nguyen HT, Loubiere A (1995) J Phys D: Appl Phys 28:774
16. Leach C, Ling Z, Freer R (2000) J Eur Ceram Soc 20:2759
17. Olsson E, Dunlop GL (1989) J Appl Phys 66:3666
18. Alamdari HD (2000) In: Varistors Prepared from Nanocrystalline Powders Obtained by High-energy Ball Milling, Ph.D. Thesis, laval university, Canada, p 212